Multi-area Generation-reserve Joint Dispatch Approach Considering Wind Power Cross-regional Accommodation

Ming Zhou, *Senior Member*, *CSEE*, *Member*, *IEEE*, Mu Wang, Jianfeng Li, and Gengyin Li, *Senior Member*, *CSEE*, *Member, IEEE*

***Abstract*—This paper presents a study on how to accommodate wind power into multiple regions, while simultaneously implementing economic and reliable dispatch for multi-area power system operation. The focus is on quantifying the operational risk brought by wind power uncertainty and at the same time accommodating wind power by coordinating multi-area generation and reserve resources. The reserve requirement of each area is calculated based on two indexes, namely, loss of load probability and wind spillage probability. Then, a generation-reserve co-optimization dispatch model that factors cross-regional wind power accommodation is proposed. The transmission margin and network security constraints of tie-lines are considered to systematically allocate reserve resources for all areas. Finally, optimality condition decomposition is used to decompose the dispatching model to achieve relatively independent regional scheduling, and to get the global optimization result. The reasonableness and effectiveness of the proposed approach is validated by a 6-bus 2-area test system and a 236-bus interconnected system.**

***Index Terms*—Cross-regional scheduling, decomposition and coordination, network security constraints, reserve optimization, wind power accommodation.**

I. INTRODUCTION

WITH the rapid growth of wind energy penetration into the grid, the intrinsic characteristics of wind power, such as randomness and volatility have brought challenges to the security and economy of power system operation. To maintain reliable wind power integrated power systems operations, adequate reserve is necessary for the power system to cope with all types of uncertainties [1]. Currently, the interconnected power system has become the main platform for optimal allocation of resources. In this scenario, cross-regional accommodation of wind power has emerged as an important research issue, particularly since the wind resource is typically far away from the load center, therefore is difficult to be consumed locally [2]. This problem has given rise to the research area of multi-area generation-reserve joint optimization dispatch, which studies cross-regional wind power accommodation. In this paper, we will investigate three aspects related to reserve optimization: first, how to quantify the required reserve for each area according to the operation risks related to wind power fluctuation; second, how to jointly allocate generation and reserve across the regions to promote wind power accommodation via reserve assistance from adjacent regions; third, how to develop an effective algorithm that can solve the high dimensional joint dispatch model for wind power integrated multi-area power systems.

The determination of reserve demand is a compromise between operation cost and reliability. Both deterministic and probabilistic methods have been applied to establish reserve requirements. The deterministic approach sets spinning reserve to a predefined amount, such as equaling to the capacity of the largest committed unit, or to some fraction of the peak load, or to some portion of the maximum wind power, or to a combination of these guidelines. Although these techniques can be understood and implemented easily, they tend to ignore the complexity of power system operations.

Probabilistic techniques, on the other hand, provide a comprehensive and realistic evaluation to the risk because they incorporate the stochastic nature of the system operation [4], [5]. Two methodologies, namely, statistic-based (only performing statistical analysis without solving the optimization problem) and optimization-based (additionally solving the optimization problem) are typically employed in the probabilistic reserve provision [6]. The statistic-based reserve determination requires statistical assessment to all drivers making imbalance between generation and consumption so that a target risk level is ultimately satisfied [7]–[9]. Contrary to the statistic-based reserve determination method, in some optimization-based methodologies, the reliability indices (e.g., in [10], [11]) or the risk index (e.g., in [12]) combined with the system conditions are provided by an analytical function form and incorporated into the constraints of unit commitment (UC). Then the optimal economic dispatching scheme is achieved by solving this optimization problem under a predefined reliability level.

Manuscript received August 3, 2016; revised September 4, 2016; accepted September 19, 2016. Date of publication March 30, 2017; date of current version December 27, 2016. This work was supported in part by the National Key Research and Development Program (2016YFB0900105) and the National Natural Science Foundation of China (51577061) and the Management & Consultation Project of SGCC.

M. Zhou (corresponding author, e-mail: zhouming@ncepu.edu.cn) and G. Y. Li are with the State Key Laboratory for Alternate Electrical Power System with Renewable Energy Sources, North China Electric Power University, Beijing 102206, China.

M. Wang is with the North China Power Engineering Co., Ltd. of China Power Engineering Consulting Group, Beijing 100011, China.

J. F. Li is with China Electric Power Research Institute, Beijing 100092, China.

DOI: 10.17775/CSEEJPES.2017.0010

In other optimization-based methodologies, the stochastic optimization method is used, that is, the corresponding probability in the future are given under all possible scenarios; here the system's expected operation cost tends to be minimized and the optimal reserve quantity and its configuration scheme are acquired by solving the optimization problem.

In most cases of co-optimization of generation and reserve, the wind power integrated system is usually treated as a single system [13], [14]. Only a few studies consider wind accommodation by dispatching generation and reserve in the multi-area interconnected system [15]–[17]. A chance constrained model considering the characteristics of reserve resources in each sub-system is built up in [15] to quantify the reserve support by adjacent subsystems to the sub-system with wind power. A zonal reserve model in the power market is built in [16]. The generation-reserve co-optimization method in multi-area power systems towards risk precaution targets based on stochastic optimization is studied in [17] to rationally configure reserve resources on the space. However, all these studies assume that the regional information is fully available across the whole system. In fact, a multi-area power system is usually dispatched regionally and independently under the premise of keeping the interconnected exchange agreement, which brings challenges to wind power cross-regional accommodation.

Given the above background, coordinated optimization is regarded as an effective method to solve the generation-reserve joint optimization dispatch problem. In [18]–[20], the Lagrangian relaxation method is introduced into UC. In [21], the augmented Lagrange algorithm is applied to solve the multi-area stochastic UC by constructing a virtual node on the tie-line. In [22] the decomposed calculation of the state estimation problem is achieved using the optimality condition decomposition (OCD) method, and the fast convergence principle is displayed in the system architecture. The OCD method is proposed in [23] to solve the multi-area optimal power flow problems, fully verifying that the OCD method is simple and effective, and can avoid some problems, such as convergence speed depending too much on the choice of some parameters, or the intervention of coordination layers necessary for updating the information.

Inspired by [23], a generation-reserve coordinated optimization dispatch approach for a multi-area wind power integrated system is proposed based on the OCD algorithm in this paper. The contributions of this paper are as follows:

1) A decomposition coordination optimization model is adopted to maintain regional scheduling's relative independence, and at the same time to achieve the global optimization, which is more suitable for the "hierarchical partition dispatching mode" in China. Decomposed calculations can be accomplished in parallel with higher computation efficiency.
2) Two indices: loss of load probability (LOLP) and wind spillage probability (WSP) are introduced, and the quantitative formulas between these indices and the operating reserve requirement for each area are established.
3) Wind power cross-regional accommodation is realized by considering the tie-lines' dual responsibilities of both power transmission and reserve assistance from neighboring areas.
4) Two case studies: a 6-bus two-area system and a 236-bus interconnected system are used to verify that the co-optimization model and the coordination algorithm can achieve optimal generation and reserve configuration in multi-area interconnected systems at the same time to improve both wind power accommodation and economy of whole system operations.

This paper is organized as follows. Reserve determination based on probability indexes is deduced in Section II. A generation-reserve co-optimization dispatch model is presented in Section III wherein a decomposed and coordinated optimization algorithm based on the OCD method is followed. Case studies are given in Section V, and conclusions are presented in Section VI.

II. Reserve Determination Based on Probability Indexes

The uncertainties of wind power and load are the key factors related to reserve determination. Since the distribution of prediction errors of load and wind power do not affect our proposed method, for simplicity, we assume that prediction errors of wind power and load follow zero-mean normal distributions. The wind power forecast error is denoted by ΔP_t^{W}, assuming its probability density function is $f(\Delta P_t^{\mathrm{W}}) \sim N(0, w_t^2)$. Similarly, the load forecast error is denoted by ΔP_t^{D} assuming its probability density function is $f(\Delta P_t^{\mathrm{D}}) \sim N(0, d_t^2)$. Then if wind power forecast and load forecast are denoted by $P_t^{\mathrm{W_0}}$ and $P_t^{\mathrm{D_0}}$, respectively, and since the practical wind power and load are random variables, then they can be expressed as $P_t^{\mathrm{W}} = P_t^{\mathrm{W_0}} + \Delta P_t^{\mathrm{W}}$ and $P_t^{\mathrm{D}} = P_t^{\mathrm{D_0}} + \Delta P_t^{\mathrm{D}}$. For convenience, we introduce net load forecast error, which is defined by $\Delta P_t^{\mathrm{N}} = \Delta P_t^{\mathrm{D}} - \Delta P_t^{\mathrm{W}}$; then its probability density function is $f(\Delta P_t^{\mathrm{N}}) \sim N(0, w_t^2 + d_t^2)$ since wind power and load are independent of each other.

Wind power forecast error, load forecast error, and failures of generations and lines are the main uncertainties that may result in operational risk, such as load shedding or wind curtailment. Therefore, two indexes, LOLP and WSP, are proposed to describe the above system risk.

Load shedding may happen under events, such as wind power prediction on the high side and load prediction on the low side at same time as the occurrence of outage of conventional generators. The situation of no generator shutdown or only one generator shutdown is taken into consideration, and the calculation of loss of load probability in period t denoted by p_t^{LOLP} is given by

$$\begin{aligned} p_t^{\mathrm{LOLP}} = & \prod_{i}^{\Omega} (1 - p_{i,\mathrm{out}}^{\mathrm{G}}) \cdot p\{(\Delta P_t^{\mathrm{N}} - R_t^{\mathrm{U}}) > 0\} \\ & + \sum_{i=1}^{\Omega} p_{i,\mathrm{out}}^{\mathrm{G}} \cdot \prod_{\substack{j=1 \\ j \neq i}}^{\Omega} (1 - p_{j,\mathrm{out}}^{\mathrm{G}}) \\ & \cdot p\{(\Delta P_t^{\mathrm{N}} + P_{i,\max}^{\mathrm{G}} - R_t^{\mathrm{U}}) > 0\} \end{aligned} \quad (1)$$

where Ω is the set of conventional generators in the researched area, $p^{\mathrm{G}}_{i,\mathrm{out}}$ is the forced outage rate of unit i, R^{U}_t is up reserve requirement, and $P^{\mathrm{G}}_{i,t}$ is power output of unit i at period t. It is worth noting that the forced outage probability at the same time of two or more generators is too small to be considered.

Wind curtailment happens under events, such as wind power prediction on the low side while load prediction is on the high side. The calculation of wind spillage probability in period t denoted by p^{WAP}_t is given by

$$p^{\mathrm{WAP}}_t = p\{(\Delta P^{\mathrm{N}}_t + R^{\mathrm{D}}_t) < 0\} \tag{2}$$

where R^{D}_t represents down reserve requirement for the area.

For a power system without wind power integration, the net load forecast error only contains the load forecast error.

If the distribution function of the net load forecast error ΔP^{N}_t is denoted by $F_{\mathrm{N}}(\cdot)$, then (1) and (2) can be modified as

$$\begin{aligned} p^{\mathrm{LOLP}}_t = &\prod_{i}^{\Omega}(1-p^{\mathrm{G}}_{i,\mathrm{out}})\cdot[1-F_{\mathrm{N}}(R^{\mathrm{U}}_t)] \\ &+\sum_{i=1}^{\Omega}p^{\mathrm{G}}_{i,\mathrm{out}}\cdot\prod_{\substack{j=1\\ j\neq i}}^{\Omega}(1-p^{\mathrm{G}}_{j,\mathrm{out}}) \\ &\cdot[1-F_{\mathrm{N}}(R^{\mathrm{U}}_t - P^{\mathrm{G}}_{i,\max})] \end{aligned} \tag{3}$$

$$p^{\mathrm{WAP}}_t = F_{\mathrm{N}}(-R^{\mathrm{D}}_t). \tag{4}$$

Assuming p^{LOLP}_0 and p^{WAP}_0 represents the required loss of load probability and the required wind spillage probability, respectively, then the reliability constraints should be met as follows:

$$p^{\mathrm{LOLP}}_t \le p^{\mathrm{LOLP}}_0 \tag{5}$$

$$p^{\mathrm{WAP}}_t \le p^{\mathrm{WAP}}_0. \tag{6}$$

Here p^{LOLP}_0 and p^{WAP}_0 can be converted to the method of annual least total cost by the system dispatch department, and usually takes a value between 0–0.1 [11]. Given the above two required values, substitute the specific expressions of (3) and (4) into (5) and (6), then the required reserve capacity R^{U}_t and R^{D}_t can be calculated based on the desired reliability level.

III. Centralized Generation-reserve Co-optimization Dispatch Model

Based on the inseparable relationship between reserve allocation and generation schedule, generation and reserve are jointly dispatched in this paper. Thus, considering the co-optimization of generation and reserve, a cross-regional optimization dispatch model for multi-area interconnected power systems with wind power integration is proposed. Through the proposed method, generation schedule, reserve configuration, and an inter-regional power transfer plan are given simultaneously.

A. Objective Function

The objective function for an interconnected system with wind power integration is to minimize the total operation cost. For each sub-region, the operation cost is described as follows.

1) Generation Cost

$$C_1 = \sum_{t\in T}\sum_{i\in\Omega^m}\gamma^m_{i,t}f_i(P^{\mathrm{G}m}_{i,t}) \tag{7}$$

where t is index of time periods from 1 to T, M is the subarea set of the interconnected system, Ω^m is the set of conventional generators of area m which belongs to M, $\gamma^m_{i,t}$ is the on/off binary variable for the commitment of the units, and $P^{\mathrm{G}m}_{i,t}$ is the power committed for generator i at period t in area m. In a unit commitment problem, generation cost function is usually described as

$$f(P^{\mathrm{G}m}_{i,t}) = a_i + b_i P^{\mathrm{G}m}_{i,t} + c_i(P^{\mathrm{G}m}_{i,t})^2 \tag{8}$$

where a_i, b_i, and c_i are constants.

2) Start-up Cost

$$C_2 = \sum_{t\in T}\sum_{i\in\Omega^m}\gamma^m_{i,t}(1-\gamma^m_{i,t-1})C^{\mathrm{st}}_{i,t} \tag{9}$$

Here the start-up cost of unit i can be described as

$$C^{\mathrm{st}}_{i,t} = \begin{cases} C^{\mathrm{hot}}_i, & T^{\mathrm{off}}_i \le t^{\mathrm{off}}_{i,t} \le T^{\mathrm{off}}_i + T^{\mathrm{cold}}_i \\ C^{\mathrm{cold}}_i, & t^{\mathrm{off}}_{i,t} \ge T^{\mathrm{off}}_i + T^{\mathrm{cold}}_i \end{cases} \tag{10}$$

where C^{hot}_i and C^{cold}_i are warm and cold start-up costs, respectively, T^{off}_i and T^{cold}_i are the minimum shut-down time and cold start-up time, respectively, and $t^{\mathrm{off}}_{i,t}$ is the actual shut-down time. The shut-down cost is negligible because of its small value.

3) Reserve Cost

$$C_3 = \sum_{t\in T}\sum_{i\in\Omega^m}\gamma^m_{i,t}f(R^{\mathrm{U}m}_{i,t}, R^{\mathrm{D}m}_{i,t}) \tag{11}$$

where the reserve cost of unit i can be described as

$$f(R^{\mathrm{U}m}_{i,t}, R^{\mathrm{D}m}_{i,t}) = C^{\mathrm{U}m}_{i,t}R^{\mathrm{U}m}_{i,t} + C^{\mathrm{D}m}_{i,t}R^{\mathrm{D}m}_{i,t} \tag{12}$$

where $C^{\mathrm{U}m}_{i,t}$ and $C^{\mathrm{D}m}_{i,t}$ are the up and down reserve prices at period t in area m, respectively, $R^{\mathrm{U}m}_{i,t}$ and $R^{\mathrm{D}m}_{i,t}$ are the scheduled up and down spinning reserve amount, respectively.

4) Load Shedding Cost

$$C_4 = \sum_{t\in T}\sum_{n\in N^m}C^{\mathrm{DS}m}_t P^{\mathrm{DS}m}_{n,t} \tag{13}$$

where $P^{\mathrm{DS}m}_{n,t}$ is the lost load of bus n in area m at period t, N^m is the bus set of area m, and $C^{\mathrm{DS}m}_t$ is the unit load shedding cost in area m at period t. As to load shedding cost, since there is no unified standard in the industry, this can be estimated through loss statistics, input-output analysis, or questionnaires. To avoid huge losses to the users and society due to unnecessary load shedding measures, it is reasonable to set a larger value to the unit load shedding cost.

5) Wind Curtailment Cost

$$C_5 = \sum_{t\in T}\sum_{j\in W^m}C^{\mathrm{WS}m}_t P^{\mathrm{WS}m}_{j,t} \tag{14}$$

where $P^{\mathrm{WS}m}_{j,t}$ is the amount of wind curtailment of wind plant j in area m at period t, W^m is the set of wind plants for area m, and $C^{\mathrm{WS}m}_t$ is the unit wind curtailment cost in area m at period t. To avoid unnecessary wind curtailment, it is reasonable to set a larger value for the unit wind curtailment cost.

So, the whole objective function can be described as

$$\min\sum_{M}(C_1+C_2+C_3+C_4+C_5). \tag{15}$$

B. Constraints

1) Power Balance Constraints for Each Bus

A reference bus is designated in a proper sub-area in a DC flow model. The power balance equation for any bus in area m at period t is as follows:

$$\sum_{i\in\Omega_n^m} P_{i,t}^{\mathrm{G}m} + \sum_{j\in W_n^m} (P_{j,t}^{\mathrm{W}m} - P_{j,t}^{\mathrm{WS}m}) - (P_{n,t}^{\mathrm{D}m} - P_{n,t}^{\mathrm{DS}m}) - \sum_{p\in N_n^m} P_{np,t}^{\mathrm{L}m} - \sum_{r\in B_n^m} P_{nr,t}^{\mathrm{T}m} = 0 \tag{16}$$

where Ω_n^m and W_n^m are the set of conventional generators and wind plants at bus n in area m, N_n^m and B_n^m are the set of buses connected to interior bus n in area m and external buses in neighboring areas connected to border bus n in area m, $P_{j,t}^{\mathrm{W}m}$ and $P_{n,t}^{\mathrm{D}m}$ are wind power forecast of wind plant j and load forecast of bus n at period t, and $P_{np,t}^{\mathrm{L}m}$ and $P_{nr,t}^{\mathrm{T}m}$ are transmission powers of internal line *np* and tie-line *nr* of area m at period t. Meanwhile, the load shedding capacity constraints and wind curtailment capacity constraints should be met as follows:

$$0 \le P_{n,t}^{\mathrm{DS}m} \le P_{n,t}^{\mathrm{D}m} \tag{17}$$

$$0 \le P_{n,t}^{\mathrm{WS}m} \le P_{n,t}^{\mathrm{W}m}. \tag{18}$$

2) Generation Units Constraints

1) Output constraints

$$P_{i,t}^{\mathrm{G}m} + R_{i,t}^{\mathrm{U}m} \le \gamma_{i,t}^{m} P_{i,\max}^{\mathrm{G}m} \tag{19}$$

$$P_{i,t}^{\mathrm{G}m} - R_{i,t}^{\mathrm{D}m} \ge \gamma_{i,t} P_{i,\min}^{\mathrm{G}m} \tag{20}$$

where $P_{i,\max}^{\mathrm{G}m}$ and $P_{i,\min}^{\mathrm{G}m}$ are the maximum and minimum capacity of unit i, respectively.

2) Ramp constraints

$$-\Delta T r_i^{\mathrm{d}} \le P_{i,t}^{\mathrm{G}m} - P_{i,t-1}^{\mathrm{G}m} \le \Delta T r_i^{\mathrm{u}} \tag{21}$$

$$\begin{cases} R_{i,t}^{\mathrm{U}m} \le \Delta T_{\mathrm{R}} r_i^{\mathrm{u}} \\ R_{i,t}^{\mathrm{D}m} \le \Delta T_{\mathrm{R}} r_i^{\mathrm{d}} \end{cases} \tag{22}$$

where ΔT is the dispatch interval, ΔT_{R} is the reserve dispatch time, which is usually 10 m, r_i^{u} and r_i^{d} are the up and down ramp rate of unit i.

3) Reserve Constraints

For area m, the margin between the cross-regional transfer power and the transfer capacity of tie-lines is used to decide the max reserve supported by neighboring areas at a given moment. Then the reserve requirement acquired by (5) and (6) is introduced to make a decision for reserve allocation for area m.

1) Up reserve constraints

Under these conditions, the prediction of wind power is higher than the real one, the prediction of load is lower than the real one, or if any conventional generator is in outage, then the up reserve is a requisite. If the amount of up reserve provided by area m itself is not enough, the support from neighboring areas through tie-lines is needed. Thus, the up reserve decision is constrained by (23)–(25).

$$\sum_{i\in G^m} R_{i,t}^{\mathrm{U}m} + \sum_{\substack{e\in\Omega \\ e\neq m}} \sum_{r\in B^e} R_{nr,t}^{\mathrm{U}e} \ge R_t^{\mathrm{U}m} \tag{23}$$

$$\sum_{r\in B^e} R_{nr,t}^{\mathrm{U}e} \le \zeta_t^e \sum_{i\in G^e} R_{i,t}^{\mathrm{U}e} \tag{24}$$

$$R_{i,t}^{\mathrm{U}m},\ R_{i,t}^{\mathrm{U}e} \ge 0 \tag{25}$$

Here, B^e denotes the set of border buses of neighboring area e, which is connected to area m ($e \in M$ and $e \neq m$), $R_{nr,t}^{\mathrm{U}e}$ denotes the regional up reserve supported by area e through tie-line *nr* at period t, and ζ_t^e represents the permitted max rate of outward supportive reserve capacity to the reserve configuration capacity in area e.

Based on the above reserve constraints, for area m, the sum of reserve provided both by area m itself and adjacent areas, which connect to area m by tie-lines ought to be no less than the reserve requirement of area m. Meanwhile, for any adjacent area e, its outward reserve should be no more than the permitted max capacity. In addition, all reserve variables should be non-negative. Regional assistance usually happens when a given region is faced with serious failures, even though the probability of serious failures simultaneously occurring in two or more sub-regions of an interconnected system is very small. Thus this paper assumes only one sub-region needs interregional assistance at the same time.

2) Down reserve constraints

If the prediction of wind power is lower than the real one, or the prediction of load is higher, then down reserve is requisite. If the amount of down reserve provided by area m itself is not enough, the support from neighboring areas through tie-lines is needed. Thus, the down reserve decision is constrained by (26)–(28).

$$\sum_{i\in G^m} R_{i,t}^{\mathrm{D}m} + \sum_{\substack{e\in\Omega \\ e\neq m}} \sum_{r\in B^e} R_{nr,t}^{\mathrm{D}e} \ge R_t^{\mathrm{D}m} \tag{26}$$

$$\sum_{r\in B^e} R_{nr,t}^{\mathrm{D}e} \le \zeta_t^e \sum_{i\in G^e} R_{i,t}^{\mathrm{D}e} \tag{27}$$

$$R_{i,t}^{\mathrm{D}m},\ R_{i,t}^{\mathrm{D}e} \ge 0 \tag{28}$$

where $R_{nr,t}^{\mathrm{D}e}$ denotes the regional down reserve supported by area e through tie-line *nr* at period t.

The above constraints ensure that area m with a proper amount of reserve can be supported by neighboring areas in case of fluctuation of wind power and load, or emergencies of the power grid.

4) Network Security Constraints

1) Available transfer capability limitation of internal lines

$$\begin{cases} \left|P_{np,t}^{\mathrm{L}m}\right| \le P_{np,\max}^{\mathrm{L}m} \\ P_{np,t}^{\mathrm{L}m} = (\theta_{n,t}^m - \theta_{p,t}^m)/x_{np} \end{cases} \tag{29}$$

Here, $P_{np,\max}^{\mathrm{L}m}$ denotes the maximum available transfer capacity of internal line *np*, $\theta_{n,t}^m$ and $\theta_{p,t}^m$ denote the phase angles of bus n and bus p in area m, respectively, and x_{np} denotes the reactance of line *np*.

2) Available transfer capability limitation of tie-lines

The positive direction of transfer power of tie-lines is defined as outflowing from area m, while the regional reserve supported by neighboring area e is scalar and it is inflowing into area m. Thus, for area m, the available transfer capability limitation of tie-lines is as follows:

$$\begin{cases} P_{nr,t}^{\mathrm{T}m} = (\theta_{n,t}^{m} - \theta_{r,t}^{e})/x_{nr} \\ \left|P_{nr,t}^{\mathrm{T}m} - R_{nr,t}^{\mathrm{Ue}}\right| \leq P_{nr,\max}^{\mathrm{T}m} \\ \left|P_{nr,t}^{\mathrm{T}m} + R_{nr,t}^{\mathrm{De}}\right| \leq P_{nr,\max}^{\mathrm{T}m} \end{cases} \tag{30}$$

where $P_{nr,\max}^{\mathrm{T}m}$ denotes the maximum available transfer capacity of the tie-line *nr*.

In period t, the sum of reserve supported by the adjacent areas and the planned transfer power cannot exceed the limitation of the available regional transfer capability. The margin between the available regional transfer capability and the transfer plan is employed to determine the max supportive reserve capacity transmitted by the tie-line in a certain period, as shown in Fig. 1. Assuming the positive flow direction of tie-lines is from area m to area e, the up-margin between the max transfer capability and the transfer plan is determined as the threshold limit of up support reserve from area m to area e or down supportive reserve from area e to area m, corresponding to the top half of the box in Fig. 1. Similarly, the down-margin is determined as the threshold limit value of down support reserve from area m to area e or up support reserve from area e to area m, corresponding to the bottom half of the box.

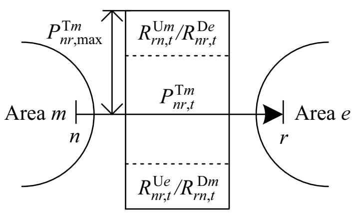

Fig. 1. The relationship between regional transmission power with the supportive reserve capacity.

To be applied to the later decomposition-coordination algorithm, constraint (30) is rewritten as the form of (31)–(33).

$$(\theta_{n,t}^{m} - \theta_{r,t}^{e})/x_{nr} - P_{nr,t}^{\mathrm{T}m} = 0 : \eta_{nr,t}^{m} \tag{31}$$

$$\begin{cases} -(\theta_{n,t}^{m} - \theta_{r,t}^{e})/x_{nr} + R_{nr,t}^{\mathrm{Ue}} \leq P_{nr,\max}^{\mathrm{T}m} : \kappa_{nr,t}^{m} \\ (\theta_{n,t}^{m} - \theta_{r,t}^{e})/x_{nr} - R_{nr,t}^{\mathrm{Ue}} \leq P_{nr,\max}^{\mathrm{T}m} : \nu_{nr,t}^{m} \end{cases} \tag{32}$$

$$\begin{cases} -(\theta_{n,t}^{m} - \theta_{r,t}^{e})/x_{nr} - R_{nr,t}^{\mathrm{De}} \leq P_{nr,\max}^{\mathrm{T}m} : \chi_{nr,t}^{m} \\ (\theta_{n,t}^{m} - \theta_{r,t}^{e})/x_{nr} + R_{nr,t}^{\mathrm{De}} \leq P_{nr,\max}^{\mathrm{T}m} : \mu_{nr,t}^{m} \end{cases} \tag{33}$$

where $\eta_{nr,t}^{m}$, $\kappa_{nr,t}^{m}$, $\nu_{nr,t}^{m}$, $\chi_{nr,t}^{m}$ and $\mu_{nr,t}^{m}$ are the Lagrange multipliers related to the boundary of area m.

IV. Decomposed and Coordinated Optimization Dispatch Model Based on the OCD Method

A. Decomposition-coordination Algorithm

The core idea of the decomposition-coordination algorithm is as follows: 1) The large-scale optimization problem of a multi-area interconnected grid is decomposed into optimization sub-problems by region; 2) The coordination is achieved by the connected relation of tie-lines, and the tie-line power flow is regarded as coupling elements between areas; 3) Each sub-problem is optimized in its own area and specific information is exchanged between adjacent regions connected by tie-lines, gradually leading to the local solution for each area approaching the global optimal solution.

Some widely used decomposition-coordination mathematical methods are classical Lagrangian relaxation (CLR), augmented Lagrangian relaxation (ALR), and optimality condition decomposition (OCD). When there are many coupling constraints in the CLR algorithm, a large number of Lagrange multipliers are prone to vibrate with poor convergence. The ALR algorithm introduces coupling constraints into the object function in the form of a quadratic term, so the problem cannot be decomposed directly unless decomposed by means of the auxiliary problem principle (APP). Meanwhile, in the computation of the ALR algorithm, Lagrange multipliers are updated via the dual gradient, but it is difficult to determine the penalty parameters and step parameters that significantly influence the convergence [24]. The OCD algorithm, which is essentially a deformation of the Lagrangian relaxation method, is simple and effective, and can avoid the above problems [23]. Taking a two-area interconnected system optimization problem as an example, the principle of the OCD algorithm is illustrated in Fig. 2.

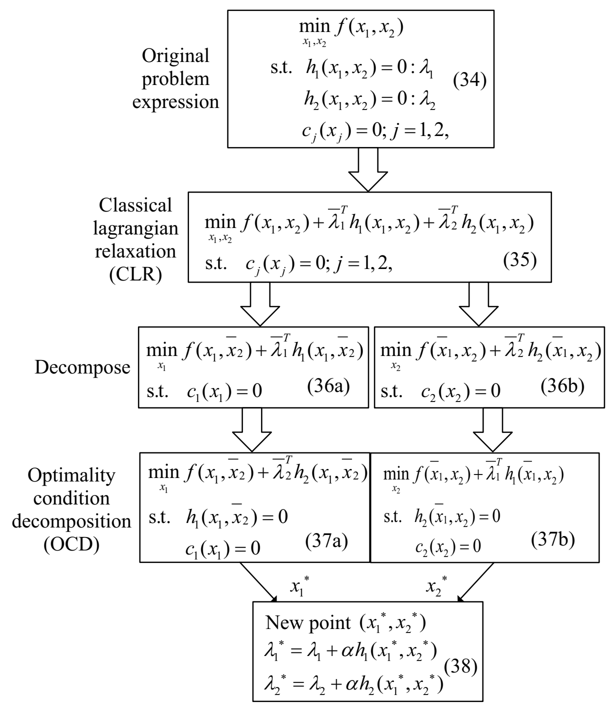

Fig. 2. Transformation of the OCD algorithm from the Lagrangian relaxation method.

As shown in Fig. 2, the objective function and constraints are indicated by (34), in which $\boldsymbol{x}_1$ and $\boldsymbol{x}_2$ are respectively decision variables set for two areas, $c_1(\boldsymbol{x}_1)$ and $c_2(\boldsymbol{x}_2)$ are constraints that contain only optimization variables of their corresponding sub-problem (i.e., simple constraints), and $h_1(\boldsymbol{x}_1, \boldsymbol{x}_2)$ and $h_2(\boldsymbol{x}_1, \boldsymbol{x}_2)$ are constraints that contain both optimization variables of two areas (i.e., complex constraints). In the Lagrangian relaxation method, simple constraints are retained while complex constraints are added into the objective function so that the original problem is rewritten as (35). The optimization problem is further decomposed into regional sub-problems. In the objective function of a sub-problem, its complex constraints are retained and variables of other regional sub-problems and Lagrange multipliers are fixed, as in (36). However, in the OCD algorithm, as shown in (37), for a sub-problem, the complex constraints of other regional sub-problems coupling with this sub-problem are added into the objective function of this sub-problem. Moreover, the complex constraints of this sub-problem are retained in the original constraints, achieving good regional independence and taking into consideration the coupling between regions. In the OCD algorithm, when regional sub-problems are solved, the corresponding Lagrange multipliers get updated in a certain way at the same time, such as seen in (38) where α is a suitable constant. The OCD algorithm depends on the following principle: the set of KKT conditions for each decomposed sub-problem is equivalent to the KKT conditions for the original problem. On the premise of a convex programming optimization problem, convergence is guaranteed by this algorithm [25].

B. Model Reconstruction

It can be noticed that the coupling variables between one area and its adjacent area exist in constraints (31)–(33), so these constraints play a key role in guaranteeing the regional coordination scheduling. This process is necessary, according to the OCD: The constraints in adjacent-area optimization problems that have coupling relationship with area m should be relaxed, and those constraints in area m to achieve decomposing a multi-area optimization problem into regional optimization sub-problems should be retained. For the optimization dispatch model of area m, the objective function is

$$\begin{aligned}\min &\sum_{m\in M}\sum_{t\in T}\sum_{i\in\Omega^m}[\gamma_{i,t}^m f(P_{i,t}^{\mathrm{G}m})+\gamma_{i,t}^m(1-\gamma_{i,t-1}^m)C_{i,t}^{\mathrm{st}}\\ &+\gamma_{i,t}^m f(R_{i,t}^{\mathrm{U}m},R_{i,t}^{\mathrm{D}m})]+\sum_{m\in\Omega}\sum_{t\in T}\sum_{n\in N^m}C_t^{\mathrm{DS}m}P_{n,t}^{\mathrm{DS}m}\\ &+\sum_{(n,r)\in\Psi^m}\tilde{\eta}_{rn,t}^e[(\tilde{\theta}_{r,t}^e-\theta_{n,t}^m)/x_{rn}-\tilde{P}_{rn,t}^{\mathrm{Te}}]\\ &+\sum_{(n,r)\in\Psi^m}\tilde{\kappa}_{rn,t}^e[-(\tilde{\theta}_{r,t}^e-\theta_{n,t}^m)/x_{rn}+\tilde{R}_{rn,t}^{\mathrm{U}m}-P_{nr,\max}^{\mathrm{Te}}]\\ &+\sum_{(n,r)\in\Psi^m}\tilde{\nu}_{rn,t}^e[(\tilde{\theta}_{r,t}^e-\theta_{n,t}^m)/x_{rn}-\tilde{R}_{rn,t}^{\mathrm{U}m}-P_{nr,\max}^{\mathrm{Te}}]\}\\ &+\sum_{(n,r)\in\Psi^m}\tilde{\chi}_{rn,t}^e[(-\tilde{\theta}_{r,t}^e-\theta_{n,t}^m)/x_{rn}-\tilde{R}_{rn,t}^{\mathrm{D}m}-P_{nr,\max}^{\mathrm{Te}}]\\ &+\sum_{(n,r)\in\Psi^m}\tilde{\mu}_{rn,t}^e[(\tilde{\theta}_{r,t}^e-\theta_{n,t}^m)/x_{rn}+\tilde{R}_{rn,t}^{\mathrm{D}m}-P_{nr,\max}^{\mathrm{Te}}]\}\end{aligned}\tag{39}$$

where ψ^m denotes the tie-line set of area m. It is important to note that $\tilde{R}_{rn,t}^{\mathrm{U}m}$ and $\tilde{R}_{rn,t}^{\mathrm{D}m}$ belong to decision variables in the optimization problem of area m.

The constraints for area m in this decomposition model is similar to the basic model presented in Section II, where (16)–(28) remain the same, while (29)–(33) are revised as

$$(\theta_{n,t}^m-\tilde{\theta}_{r,t}^e)/x_{nr}-P_{nr,t}^{\mathrm{T}m}=0:\eta_{nr,t}^m \tag{40}$$

$$\begin{cases}-(\theta_{n,t}^m-\tilde{\theta}_{r,t}^e)/x_{nr}+R_{nr,t}^{\mathrm{Ue}}\le P_{nr,\max}^{\mathrm{T}m}:\kappa_{nr,t}^m\\ (\theta_{n,t}^m-\tilde{\theta}_{r,t}^e)/x_{nr}-R_{nr,t}^{\mathrm{Ue}}\le P_{nr,\max}^{\mathrm{T}m}:\nu_{nr,t}^m\end{cases}\tag{41}$$

$$\begin{cases}-(\theta_{n,t}^m-\tilde{\theta}_{r,t}^e)/x_{nr}-R_{nr,t}^{\mathrm{De}}\le P_{nr,\max}^{\mathrm{T}m}:\chi_{nr,t}^m\\ (\theta_{n,t}^m-\tilde{\theta}_{r,t}^e)/x_{nr}+R_{nr,t}^{\mathrm{De}}\le P_{nr,\max}^{\mathrm{T}m}:\mu_{nr,t}^m\end{cases}\tag{42}$$

where the symbols with "$\sim$" indicate the decision variables; Lagrange multipliers belonging to adjacent areas are set to specified values. The specified values are determined depending on the solutions of adjacent-area sub-problems in the latest iteration and are exchanged among the sub-problems.

C. Algorithm Implementation Process

As to the coupling variables and Lagrange multipliers, the following aspects in the implementation process of the decomposition-coordination algorithm need to be considered:

1) Initialization

It is worth noting that the convergence behavior of the algorithm is directly influenced by the way in which the border bus states are initialized. Thus, it is advantageous to ignore the coordination at the first iteration, that is, each area has its own balancing bus to achieve independent optimization for each area at the first iteration. In subsequent iterations, the same balance bus (reference bus) is shared by all the interconnected areas. The independent optimization results for each area are given to determine and modify the coupling variables and Lagrange multipliers. Using the local solutions of adjacent regions, which is related to regional relative position, this method can avoid conflicts between the initial values of different areas and enhance the convergence properties of the decomposition-coordination algorithm.

2) Update

In the process of iteration, the Lagrange multipliers and coupling variables get updated and solutions for each sub-problem gradually converge to the global optimal solution. For the OCD algorithm, the coordination layer only needs to collect the information and check the convergence without any calculation of the variables or multipliers. If the process is coordinated by the sub-problems and the information is updated in the interaction, then the coordination level can be omitted, realizing fully distributed decomposed-coordinated calculations.

3) Iteration

The coordinated scheduling for the multi-area interconnected system is achieved through the exchange of information between areas. The coupling variables of boundary buses and Lagrange multipliers are regarded as the exchange information, e.g., the optimization results of area e at the ρ-th iteration is delivered as constants to the optimization problem of area m at the $(\rho+1)$-th iteration, expressed as

$$\begin{cases}(\tilde{\theta}_{r,t}^e)^{\rho+1}=(\theta_{r,t}^e)^\rho\\ (\tilde{P}_{nr,t}^{\mathrm{Te}})^{\rho+1}=(P_{nr,t}^{\mathrm{Te}})^\rho\\ (\tilde{R}_{nr,t}^{\mathrm{U}m})^{\rho+1}=(R_{nr,t}^{\mathrm{U}m})^\rho\\ (\tilde{R}_{nr,t}^{\mathrm{D}m})^{\rho+1}=(R_{nr,t}^{\mathrm{D}m})^\rho\end{cases}\quad\begin{cases}(\tilde{\eta}_{nr,t}^e)^{\rho+1}=(\eta_{nr,t}^e)^\rho\\ (\tilde{\kappa}_{nr,t}^e)^{\rho+1}=(\kappa_{nr,t}^e)^\rho\\ (\tilde{\nu}_{nr,t}^e)^{\rho+1}=(\nu_{nr,t}^e)^\rho\\ (\tilde{\chi}_{nr,t}^e)^{\rho+1}=(\chi_{nr,t}^e)^\rho\\ (\tilde{\mu}_{nr,t}^e)^{\rho+1}=(\mu_{nr,t}^e)^\rho\end{cases}\tag{43}$$

Considering the sequence between the sub-problem computation and information interaction, serial and parallel iterations are two modes of iterative methods. According to the importance of information feedback in time, the serial iterative method is adopted in this paper.

4) Convergence

In two adjacent iterations, if the decision variables and

Lagrange multipliers of all the sub-problems are changed by a small quantity, or all the constraints are satisfied by the current solutions, then the optimization problem is seen converged. The convergence condition is expressed as

$$\begin{aligned}\varepsilon = \sum_{m\in\Omega}\sum_{t\in T}\sum_{(n,r)\in\Psi^m} & [|(\eta^m_{nr,t})^\rho - (\eta^m_{nr,t})^{\rho-1}| \\ & + |(\kappa^m_{nr,t})^\rho - (\kappa^m_{nr,t})^{\rho-1}| + |(\nu^m_{nr,t})^\rho - (\nu^m_{nr,t})^{\rho-1}| \\ & + |(\chi^m_{nr,t})^\rho - (\chi^m_{nr,t})^{\rho-1}| + |(\mu^m_{nr,t})^\rho - (\mu^m_{nr,t})^{\rho-1}|] \\ \le \varepsilon_0 & \end{aligned} \tag{44}$$

where ε_0 is the set convergence tolerance.

V. Illustrative Example and Case Study

To illustrate the effectiveness of the proposed multi-area decomposition-coordination optimization dispatch approach, a 6-bus, 2-area test system and a 236-bus interconnected system consisting of two IEEE-118 subsystems are tested. The simulations are carried out using MATLAB 2010 and the mixed integer programming solver MOSEK on a Lenovo ThinkPad T440s with Intel Core i7 processors running at 2.1 GHz and 8 GB of RAM.

A. Six-bus, Two-area Test System

1) System Parameters

To illustrate the effectiveness of the proposed model, a test system in which area A and area B are connected is considered. The network parameters are modified from [26], depicted in Fig. 3, in which WP represents the wind power plant. Data for the conventional generating units of area A are given in Appendix Table I, and the unit technical parameters of area B are all the same as A, but the cost parameters of area B are twice as those of A. Reactance of the internal lines and the tie-line are all set to 0.13 p.u., while the transfer capacity is set to 0.6 and 0.45, respectively, on a base of 100 MVA. The system is tested for a five-period dispatching horizon and each period is 0.5 h. Prediction data for wind power and load are given in Appendix Table II. The forced outage rates for all conventional generators are set to 0.002. The criteria for loss of load probability and wind spillage probability are both set to 0.05.

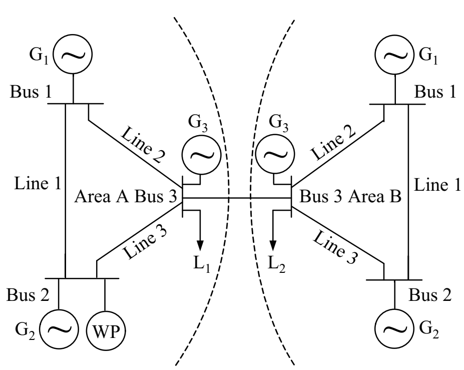

Fig. 3. The six-bus two-area test system.

2) Decomposed and Coordinated Optimization Dispatch Results

Table I and Table II list the optimal scheduling results, including the detailed generation, the cross-regional transmission powers, and spinning reserve for each control zone. Only the generators that have been committed during the scheduling horizon are listed in the tables, and the transfer power of the tie-line denoted by T_AB is flowing from area A to area B. Note that no load shedding and no wind spillage occurs during the entire scheduling horizon.

TABLE I
The Optimal Scheduling Results and Cross-regional Power Transmission Plan

(in MW)

Object	Time	1	2	3	4	5
Area A	G_1	10.0	30.0	60.0	30.0	10.0
	G_2	0.0	0.0	0.0	0.0	0.0
	G_3	40.0	49.1	50.0	40.0	41.0
Area B	G_1	10.0	15.9	39.2	17.0	47.0
	G_2	10.0	10.0	10.0	10.0	17.0
	G_3	25.0	40.0	40.8	28.0	40.0
Tie-line	T_AB	45.0	44.1	40.0	45.0	16.0

TABLE II
Reserve Coordinated Configuration Through Areas

(in MW)

Object	Time		1	2	3	4	5
A	G_1	R^{U}	10.0	10.0	10.0	10.0	10.0
		R^{D}	0.0	5.9	4.2	9.4	0.0
	G_3	R^{U}	10.0	0.9	0.0	10.0	8.9
		R^{D}	10.0	10.0	10.0	10.0	10.0
B	G_1	R^{U}	10.0	10.0	10.0	10.0	10.0
		R^{D}	0.0	0.0	0.0	0.0	3.9
	G_2	R^{U}	1.8	10.0	10.0	4.4	10.0
		R^{D}	0.0	0.0	0.0	0.0	0.0
	G_3	R^{U}	10.0	10.0	9.2	10.0	10.0
		R^{D}	6.8	0.0	0.0	0.0	10.0

In the dispatching mode related to cross-regional wind power accommodation, the tie-lines undertake the responsibility of both power transmission and reserve support from neighboring areas. Table I and Table II show that with wind power integration, the output of wind power can replace some conventional generation, and total coal consumption of the interconnected system is decreased through cross-regional power transmission. Meanwhile, the reserve requirement of the given area in any random scenario can be met by the reserve provided by units in the given area and by units in neighboring areas as well. Thus, the total reserve configuration capacity is decreased, which means that the efficient use of energy of the interconnected system is promoted.

3) Advantage of the Proposed Cross-area Dispatch Method

Taking the fourth period as an example, Table III compares the dispatch results of the proposed method with the isolated dispatch method (here the isolated dispatch means no power exchange between two areas). Then the former sets tile-line capacity to 45 MW and the latter sets tie-line capacity to 0 MW. The benefits of the interconnection are illustrated in Table III. Due to interconnection through tie-lines, not only can some expensive generating units be partly covered, but also the total reserve configuration capacity is decreased so that the total operation cost is also reduced. In the meantime, through joint optimization of generation and reserve resources from the range of the interconnected system, wind power accommodation is promoted on a larger scale.

TABLE III
COMPARISON OF DISPATCH RESULTS: INTERCONNECTED TO ISOLATED OPERATION

Method	Parameters	Area A	Area B	System Wide
Interconnected accommodation	Unit output (MW)	70	55	125
	Up reserve (MW)	20	24.4	44.4
	Down reserve (MW)	19.4	0	19.4
	Wind curtailment (MW)	0	–	0
	Tie-line power transmission (MW)	A→B		45
	Total cost ($)	30,919.1		
Isolated operation	Unit output (MW)	49.4	100	149.4
	Up reserve (MW)	44.4	27.4	71.8
	Down reserve (MW)	19.4	2.4	21.8
	Wind curtailment (MW)	24.4	–	24.4
	Tie-line power transmission (MW)	–		0
	Total cost ($)	59,434.7		

4) Comparison of Decomposition-coordination Algorithm and Centralized Algorithm

The results of the decomposition-coordination algorithm fully coincide with the results of the centralized algorithm after 12 iterations; all quantities of interest (i.e., unit outputs and reserve dispatch, tie-line and internal line power flows, etc.) converge within a $\varepsilon = 10^{-2}$ tolerance to the centralized solution. The comparison of total cost, CPU time, and iteration times between the centralized and the decentralized algorithm is reported in Table IV.

TABLE IV
COMPARISON BETWEEN THE CENTRALIZED AND DECENTRALIZED MODELS (FOR THE SIX-BUS SYSTEM)

Algorithm	Total Cost ($)	CPU Time (s)	Number of Iteration
Centralized algorithm	49,461.54	0.72	1
Decomposition-coordination algorithm	49,468.73	2.70	12

Fig. 4 shows the evolution of the tie-line flow at the peak time period as it approaches the tie-line capacity limit from both directions during the iterative procedure.

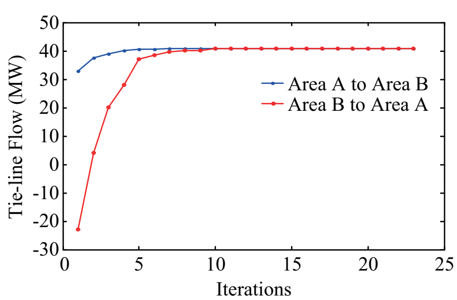

Fig. 4. Relationship of the tie-line flow with iteration times at the peak time period.

It is important to note that according to the results of this small example, the decomposition-coordination approach is able to realize decomposition calculation, and to achieve the global optimal result while maintaining regional independent scheduling; however, the computational efficiency advantage is not reflected. Thus the application of the proposed model to a larger-scale system is the next test.

B. 236-Bus Interconnected System

1) System Parameters

The 236-bus test system consists of two alike IEEE-118 systems interconnected by one 1500 MW tie-line. The two IEEE-118 systems are denoted by A and B, respectively, whose network topology and unit parameters are derived from the IEEE standard test system data. The system parameters in the software package, MatPower [27], are adopted here. Three 600 MW wind plants are linked to bus 9, 21, and 41 of area A, respectively, while area B is without wind integration. This case is tested for a five-period dispatching horizon and each period is 1 h. Prediction data for wind power and load are given in Fig. A1 in the Appendix.

2) Comparison of Decomposition-coordination Algorithm with Centralized Algorithm

The decomposition-coordination algorithm and the centralized algorithm are respectively employed to solve the generation-reserve optimization dispatch model. Table V provides the total cost, CPU time, and iteration times for both algorithms for two different values of tolerance. The total cost difference between the centralized and the decentralized solutions is 0.28% and 0.15% for tolerances of $\varepsilon = 10^{-2}$ and $\varepsilon = 10^{-4}$, respectively. As expected, the smaller value of the tolerance, on the one hand, results in better accuracy (i.e., lower cost difference), but on the other hand, requires more iterations to converge.

TABLE V
COMPARISON BETWEEN THE CENTRALIZED AND DECENTRALIZED MODELS (FOR THE 236-BUS SYSTEM)

Algorithms	Tolerance	Total Cost ($)	CPU Time (s)	Number of Iterations
Centralized algorithm	–	11,324,000	13.5	1
Decomposition-coordination algorithm	$\varepsilon = 10^{-2}$	11,356,000	42.7	41
	$\varepsilon = 10^{-4}$	11,341,000	73.4	83

To validate the effectiveness of the proposed decomposition-coordination optimization approach applied to large-scale interconnected systems, cases for a few large-scale interconnected systems are tested, as presented in Table VI. The calculation of each subsystem can use its own processor. As such it is different from the sum calculation time. The average calculation time of the proposed decomposition-coordination algorithm implies the average CPU running time on the respective optimization platform for each sub-problem, while the average calculation time of the centralized algorithm, that is the calculation time, implies the CPU running time on the whole optimization platform for the interconnected system. 2A-1T stands for two areas interconnected by one tie-line, 4A-3T represents four areas interconnected by three tie-lines, etc. As shown in Table VI, the larger scale of the system results in better efficiency of the decomposition-coordination algorithm. When the connected areas reach up to four, the average calculation time of the decomposition-coordination algorithm is less than that of the centralized algorithm; thus the request for optimizing platform hardware (or memory) would be greatly reduced. It is worth mentioning that given proper iterative initial value according to historical data, the iteration times would be effectively reduced and the computational efficiency would be greatly improved.

TABLE VI
ANALYSIS OF THE DECOMPOSITION-COORDINATION COMPUTATIONAL EFFICIENCY FOR A FEW LARGE-SCALE INTERCONNECTED SYSTEMS

Object	Average Calculation Time (s)		
	2A-1T	4A-3T	6A-5T
Centralized algorithm	9.5	25.6	76.2
Decomposition-coordination algorithm	17.4	24.5	59.6

3) Relationship Between System Total Operation Cost and Tie-line Capacity

The system total operation cost varies with the change in maximum transmission capability of the tie-line, as illustrated in Fig. 5. By increasing the transmission capacity of tie-lines, the tie-line flow would gradually improve and the total operation cost would also gradually decrease. This is because higher inter-regional electricity transmission capabilities increase chances of low-cost units within the scope of the entire network to generate more power. However, when the transmission capacity of tie-lines increases to a certain value (1800 MW), the curve of the total cost is flattened out. Therefore, when considering the boundary protocol between areas, making reasonable decisions for a transfer plan is of great significance to give full play to the advantages of inter-regional accommodation.

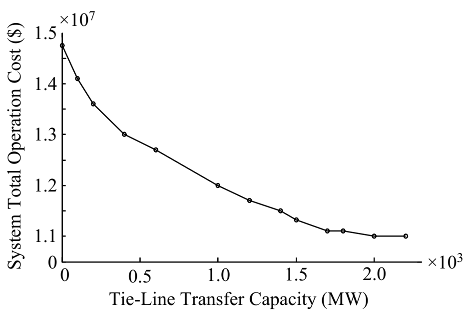

Fig. 5. The system total operation cost versus tie-line capacity.

VI. CONCLUSION

To solve the cross-regional scheduling problem for accommodating wind sources across a broader range, a decomposed and coordinated optimization dispatch model for multi-area interconnected power systems is proposed in this paper. From the theoretical properties of the proposed method and from detailed numerical simulations, the conclusions below are in order:

1) When factoring in uncertainties, such as wind power and load error predictions as well as forced outage rate of units, two indexes, namely load probability and wind spillage probability, are proposed. The quantitative relationship between these indexes and the operating reserve requirement for each area are also established.
2) Based on cross-regional reserve assistance, a generation-reserve co-optimization dispatch model that considers wind power accommodation around the interconnected system is built up.
3) A decomposed and coordinated dispatching optimization algorithm based on the optimality condition decomposition (OCD) method is proposed, which is suitable for the "hierarchical partition dispatch" set up in China. Case studies show that the proposed model and algorithm can achieve the global optimization of the multi-area power system through coordination between areas, while reducing the complexity of the solution.

APPENDIX

TABLE AI
UNIT PARAMETERS OF AREA A (FOR SIX-BUS SYSTEM)

Object	G_1	G_2	G_3
A ($/h)	100	100	100
B ($/MWh)	30	40	20
C ($/MW^{2}h)	0.3	0.8	0.2
$P_{\max}$ (MW)	100	100	50
$P_{\min}$ (MW)	10	10	10
r_{iu} (MW/min)	1	1	1
r_{id} (MW/min)	1	1	1
$C_{i\mathrm{hot}}$ ($)	60	70	50
$C_{i\mathrm{cold}}$ ($)	30	35	25
C_i^{U} ($/MWh)	15	20	10
C_i^{D} ($/MWh)	15	20	10

TABLE AII
PREDICTION DATA FOR WIND POWER AND LOAD (FOR SIX-BUS SYSTEM)

t (0.5 h)	Wind (MW)	L_1 (MW)	L_2 (MW)
1	85	90	90
2	75	110	110
3	60	130	130
4	75	100	100
5	85	120	120

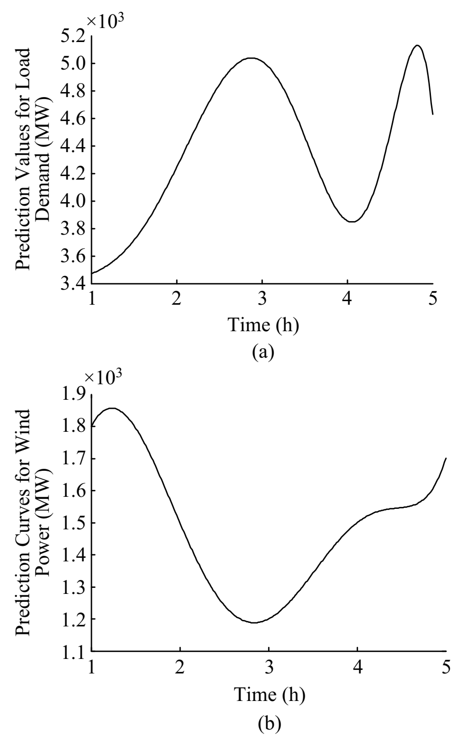

Fig. A1. Prediction curves for wind power and load demand (for 236-bus system). (a) Prediction curves for load demand. (b) Prediction values for wind power.

REFERENCES

[1] Z. Y. Xue, M. Zhou, and G. Y. Li, "Survey on reserve decision of power systems with large scale wind power integration," *Power System Protection and Control*, vol. 41, no. 4, pp. 148–155, Feb. 2013. (in Chinese)

[2] L. Z. Zhu, N. Chen, and H. L. Han, "Key problems and solutions of wind power accommodation," *Automation of Electric Power Systems*, vol. 35, no. 22, pp. 29–34, Nov. 2011. (in Chinese)

[3] M. Xiang, Z. F. Zhang, and Q. Q. Jiao, "Optimization of reserve coordination in the multi-scenario probability unit commitment for wind power integration," *Power System and Clean Energy*, vol. 28, no. 5, pp. 61–68, May 2012. (in Chinese)

[4] I. D. Margaris, S. A. Papathanassiou, N. D. Hatziargyriou, A. D. Hansen, and P. Sorensen, "Frequency control in autonomous power systems with high wind power penetration," *IEEE Transactions on Sustainable Energy*, vol. 3, no. 2, pp. 189–199, Apr. 2012.

[5] R. Allan and R. Billinton, "Probabilistic assessment of power systems," *Proceedings of the IEEE*, vol. 88, no. 2, pp. 140–162, Feb. 2000.

[6] A. Ahmadi-Khatir, M. Bozorg, and R. Cherkaoui, "Probabilistic spinning reserve provision model in multi-control zone power system," *IEEE Transactions on Power Systems*, vol. 28, no. 3, pp. 2819–2829, Aug. 2013.

[7] R. Billinton and R. N. Allan, *Reliability Evaluation of Power Systems*. New York: Springer, 1996, pp. 37–181.

[8] R. Doherty and M. O'Malley, "A new approach to quantify reserve demand in systems with significant installed wind capacity," *IEEE Transactions on Power Systems*, vol. 20, no. 2, pp. 587–595, May 2005.

[9] C. Maurer, S. Krahl, and H. Weber, "Dimensioning of secondary and tertiary control reserve by probabilistic methods," *European Transactions on Electrical Power*, vol. 19, no. 4, pp. 544–552, May 2009.

[10] D. Pozo and J. Contreras, "A chance-constrained unit commitment with a security criterion and significant wind generation," *IEEE Transactions on Power Systems*, vol. 28, no. 3, pp. 2842–2851, Aug. 2013.

[11] W. Zhou, H. Sun, H. Gu, Q. Ma, and X. D. Chen, "Dynamic economic dispatch of wind integrated power systems based on risk reserve constraints," *Proceedings of the CSEE*, vol. 32, no. 1, pp. 47–55, Jan. 2012. (in Chinese)

[12] D. Chattopadhyay and R. Baldick, "Unit commitment with probabilistic reserve," in: *Power Engineering Society Winter Meeting*, *IEEE*, 2002, pp. 280–285.

[13] X. Ai and X. Liu, "Chance constrained model for wind power usage based on demand response," *Journal of North China Electric Power University*, vol. 38, no. 3, pp. 17–22, 35, May 2011. (in Chinese)

[14] M. A. Ortega-Vazquez and D. S. Kirschen, "Estimating the spinning reserve requirements in systems with significant wind power generation penetration," *IEEE Transactions on Power Systems,* vol. 24, no. 1, pp. 114–124, Feb. 2009.

[15] S. Q. Sheng, X. L. Tan, H. Li, and L. T. Fan, "Reserve capacity optimization of interconnected power grid containing wind farms," *Power System Technology*, vol. 37, no. 11, pp. 3067–3072, Nov. 2013. (in Chinese)

[16] J. X. Wang, X. F. Wang, and X. Y. Ding, "Study on zonal reserve model in power market," *Proceedings of the CSEE*, vol. 26, no. 18, pp. 28–33, Sep. 2006. (in Chinese)

[17] Y. F. Cao, Q. X. Chen, Q. Xia, J. S. Li, and Y. Hu, "Energy-reserve co-optimization in multi-area power systems towards risk precaution target," *Power System Technology*, vol. 38, no. 8, pp. 2155–2160, Aug. 2014. (in Chinese)

[18] N. J. Redondo and A. J. Conejo, "Short-term hydro-thermal coordination by Lagrangian relaxation: Solution of the dual problem," *IEEE Transactions on Power Systems*, vol. 14, no. 1, pp. 89–95, Feb. 1999.

[19] C. Yingvivatanapong, W. -J. Lee, and E. Liu, "Multi-area power generation dispatch in competitive markets," *IEEE Transactions on Power Systems*, vol. 23, no. 1, pp. 196–203, Feb. 2008.

[20] Q. Y. Jiang, B. R. Zhou, and M. Z. Zhang, "Parallel augment Lagrangian relaxation method for transient stability constrained unit commitment," *IEEE Transactions on Power Systems*, vol. 28, no. 2, pp. 1140–1148, May 2013.

[21] A. Ahmadi-Khatir, A. J. Conejo, and R. Cherkaoui, "Multi-area unit scheduling and reserve allocation under wind power uncertainty," *IEEE Transactions on Power Systems*, vol. 29, no. 4, pp. 1701–1710, Jul. 2014.

[22] E. Caro, A. J. Conejo, and R. Minguez, "Decentralized state estimation and bad measurement identification: An efficient Lagrangian relaxation approach," *IEEE Transactions on Power Systems*, vol. 26, no. 4, pp. 2500–2508, Nov. 2011.

[23] F. J. Nogales, F. J. Prieto, and A. J. Conejo, "A decomposition methodology applied to the multi-area optimal power flow problem," *Annals of Operations Research*, vol. 120, no. 1, pp. 99–116, Apr. 2003.

[24] Z. Li and H. G. Yang, "A full decomposition proximal center algorithm for decomposition and coordination of reactive power optimization," *Proceedings of the CSEE*, vol. 33, no. 1, pp. 77–83, Jan. 2013. (in Chinese)

[25] A. J. Conejo, E. Castillo, R. Minguez, and R. Garcia-Bertrand, "Decomposition techniques in mathematical programming: engineering and science applications," Springer Science & Business Media, 2006.

[26] A. Ahmadi-Khatir, A. J. Conejo, and R. Cherkaoui, "Multi-area energy and reserve dispatch under wind uncertainty and equipment failures," *IEEE Transactions on Power Systems*, vol. 28, no. 4, pp. 4373–4383, Nov. 2013.

[27] R. D. Zimmerman, C. E. Murillo-Sánchez, and R. J. Thomas, "MATPOWER: Steady-state operations, planning, and analysis tools for power systems research and education," *IEEE Transactions on Power Systems*, vol. 26, no. 1, pp. 12–19, Feb. 2011.

Ming Zhou (SM'16) received the B.S., M.S., and Ph.D. degrees in electrical engineering from North China Electric Power University, Beijing, China, in 1989, 1992, and 2006, respectively. Since 1992, she has been with the School of Electrical and Electronic Engineering, North China Electric Power University, Beijing, China, where she is currently a Professor. Her areas of interest include power system economics, power system analysis and reliability, and power system optimization operation, etc.

Mu Wang received the B.S. and M.S. degrees in School of Electrical and Electronic Engineering, North China Electric Power University. Beijing, China, in 2013, and 2016, respectively. She is with the North China Power Engineering Co., Ltd. of China Power Engineering Consulting Group. Her current interest includes wind power accommodation and power system optimization dispatch.

Jiangfeng Li received his B.S. degree from Chang'an University, Beijing, China in 2001, and B.S. degree from Beijing Jiaotong University, Beijing, China in 2006. Now he is pursuing his Ph.D. degree in North China Electric Power University. His research area is technology and economy prediction and evaluation theory and application.

Gengyin Li (SM'09) received his B.S., M.S., and Ph.D. degrees from North China Electric Power University (NCEPU), Beijing, China, in 1984, 1987, and 1996, respectively, all in electrical engineering. Since 1987, he has been with the School of Electrical and Electronic Engineering, NCEPU, Beijing, China, where he is currently a Professor. His areas of interest include power system economics, power quality analysis and control, and new transmission and distribution technologies.